JOURNAL OF MATERIALS SCIENCE 26 (1991) 2309–2312

Comparison of defect structures in homo- and hetero-epitaxial GaP, grown using excimer laser-assisted MOVPE

U. SUDARSAN*, R. DEVANATHAN*, R. SOLANKI‡
*Departments of Materials Science and Engineering ‡and Applied Physics and Electrical Engineering, Oregon Graduate Institute, 19600 NW Von Neumann Drive, Beaverton, OR 97006, USA

Defect structures in excimer laser-assisted epitaxial GaP on (1 0 0) GaP and (1 0 0) GaAs have been examined using transmission electron microscopy (TEM). It was found that the dominant defect structures in homo-epitaxy were dislocations and stacking faults whereas the major defects in hetero-epitaxy were twins. Differential plastic deformation-induced stresses are believed to be responsible for the high density of twins in hetero-epitaxy.

1. Introduction

The current trend in opto-electronics towards smaller device dimensions and higher speeds has generated considerable interest in obtaining sharper interfaces between epitaxial layers of compound semiconductors. One way of reducing the diffusion at the interface as well as stress due to thermal expansion mismatch during hetero-epitaxy of III–V compounds is by lowering the growth temperature. Several approaches have been explored to reduce the growth temperature, including the use of plasmas [1, 2] and ultraviolet (u.v.) radiation [3–8]. The secondary energy sources serve to lower the effective activation energy, hence the growth temperature. We have been investigating the latter technique to achieve both homo- and hetero-epitaxial growth of GaP [9, 10].

2. Experimental

The experimental set-up consisted of a stainless steel reactor and an excimer-laser, which was operated at 193 nm (ArF). The precursor gases for GaP were trimethylgallium (TMG) and tertiarybutylphosphine (TBP), with hydrogen as the carrier gas. The laser was focused onto the substrate which was placed on a heated susceptor in the reactor. The deposition temperature was 500 °C and the pressure was typically 1.9 kPa. The details of this reactor and growth conditions are described elsewhere [9].

For the present study, thin films of GaP were grown on (1 0 0) GaP and (1 0 0) GaAs substrates. Samples were etched with 10:1:1 H_2SO_4: H_2O: H_2O_2 for 5 min at room temperature, rinsed in deionized water and blow dried with nitrogen before being loaded in the growth chamber. The growth process was started in the presence of TBP and H_2 and then TMG was introduced. Samples were prepared for cross-section transmission electron microscopy (XTEM) using the conventional method that included mechanical grinding and ion-milling. The XTEM micrographs were examined at the hetero- and homo-interface in both the samples using four different reflections.

3. Results

In the absence of laser irradiation, growth of both homo- and hetero-epitaxial GaP were fine grained polycrystalline in nature. However, under identical conditions, with laser on (energy density of 0.11 J cm^{-2}), the deposits were epitaxial on both GaP and GaAs. The rest of the discussion will be devoted to the defect structures of the thin film GaP structures obtained under laser irradiation.

3.1. Defect structure in GaP/GaP

The defect structure of the homo-epitaxial GaP is shown in Fig. 1a–d. The XTEM sample was viewed using four different 2-beam conditions, $0\bar{2}2$, 400, $\bar{2}\bar{2}2$ and $\bar{2}2\bar{2}$ to analyse the defect structures. The ***gb*** criterion was used for visibility of dislocations, where ***g*** is the diffraction vector and ***b*** the Burgers vector of dislocations [11]. There was a high defect density region close to the interface which extended up to 0.08 μm into the epilayer (Fig. 1a). This region consisted of both line (dislocations) and planar (twins, stacking faults) defects. Above the highly defective interface region, the most dominant defect structure in the epilayer was stacking faults. The partial dislocations enclosing the stacking faults which disappeared under $[0\bar{2}2]$ beam condition had a 1/6 ⟨2 1 1⟩-type Burgers vector and are indicated by '*p*' in Fig. 1. Pure edge dislocations with Burgers vector of the type $\pm 1/2[0\bar{1}1]$ type, indicated by '*e*' were also observed in the epilayer. These became invisible under [4 0 0] reflection. The threading dislocations penetrated the epitaxial film and are indicated by '*t*' in Fig. 1d.

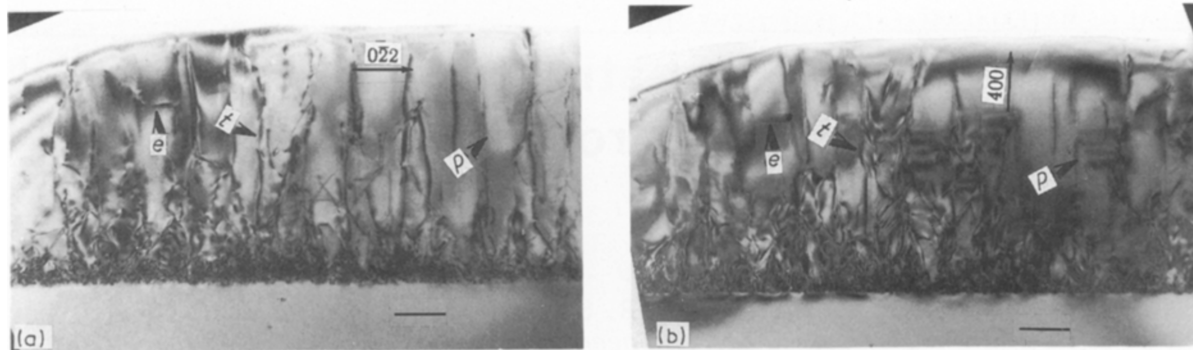

Figure 1 XTEM micrographs showing the defect structure in homo-epitaxial GaP under four different reflections: (a) $0\bar{2}2$, (b) 400, (c) $\bar{2}\bar{2}2$, and (d) $\bar{2}2\bar{2}$. In the figures, '*p*' indicates partial dislocation, '*e*', pure edge dislocation and '*t*', threading dislocation. The markers represent 0.25 μm.

3.2. Defect structure in GaP/GaAs

The defect structures observed in the hetero-epitaxial GaP on GaAs are shown in Fig. 2a–d. These micrographs were taken at four different 2-beam conditions, i.e., $[02\bar{2}]$, $[\bar{4}00]$, $[22\bar{2}]$ and $[2\bar{2}2]$. It should be noted that both the homo- and hetero-epitaxial layers were grown under identical experimental conditions.

One major difference observed in the defect structures of the homo- and hetero-epitaxial layers is the presence of twins in the latter case which is indicated by arrows in Fig. 2a–d. Although twins were also observed in the homo-epitaxial growth, they were not the dominant defect structures, whereas in the hetero-epitaxial film they extended from the interface to the top of the epilayer. From Fig. 2c and d, it is clear that twinning has occured along the four $\{111\}$ planes. The sample was tilted to reveal only the twin structure (Fig. 3) which showed that the defects originated from the interface and propagated through the film thickness.

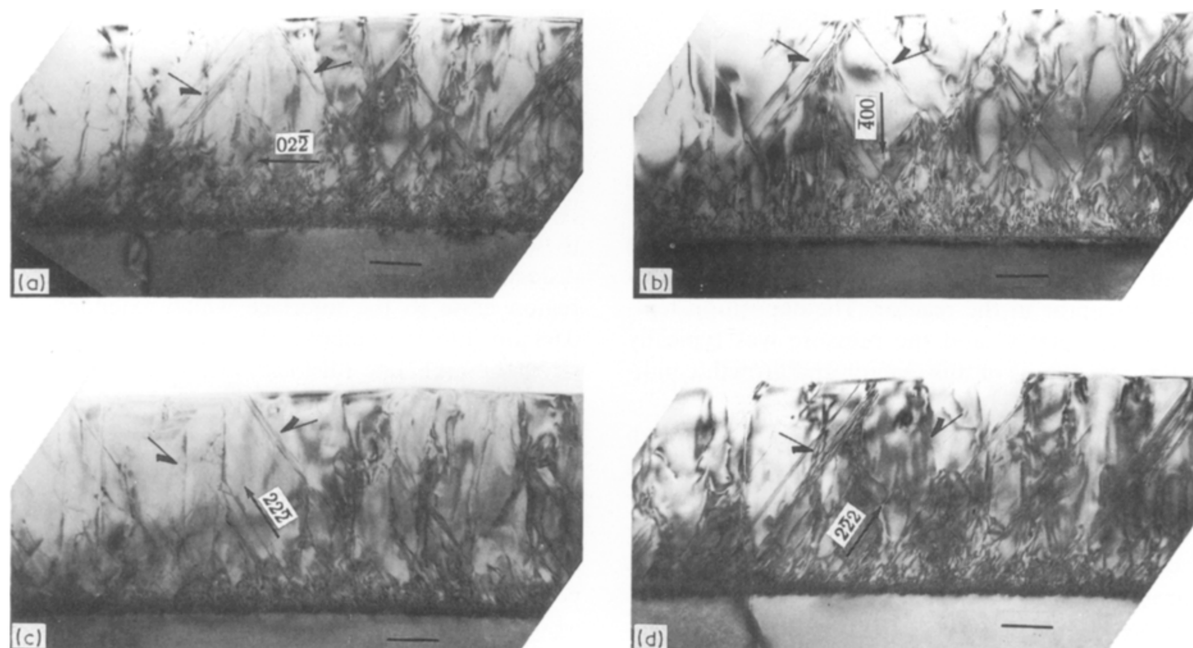

Figure 2 XTEM micrographs showing the defect structure in GaP grown on GaAs under four different reflections: (a) $02\bar{2}$, (b) $\bar{4}00$, (c) $22\bar{2}$, and (d) $2\bar{2}2$. The arrows indicate twins. The markers represent 0.25 μm.

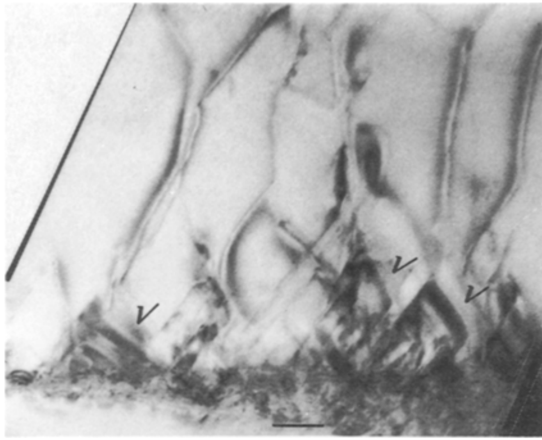

Figure 3 Hetero-epitaxial GaP sample tilted to reveal twins. The marker represents 0.25 μm.

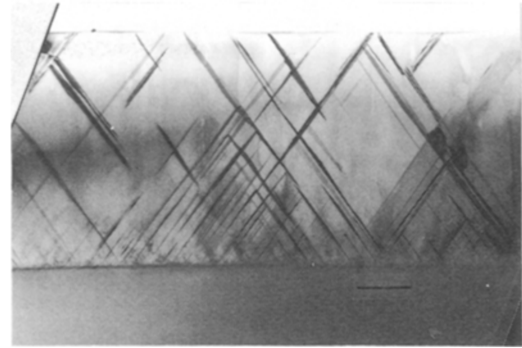

Figure 4 XTEM micrograph of GaP/GaAs tilted to reveal the interface. The marker represents 0.025 μm.

There was also a conspicuous absence of the partial dislocations enclosing the stacking faults under $[22\bar{2}]$ and $[2\bar{2}2]$ beam conditions (Fig. 2c and d). In order to further examine the interface, the XTEM sample was tilted which revealed the presence of triangular structures that could be the pyramid-shaped dislocation tangles (PDT) [12, 13]. Dislocations originated from the apex of these triangular structures (Fig. 4). The presence of these defects has been attributed to composition inhomogeneities at the interface and 3-D island formation during the nucleation stage of the film growth process [13]. In contrast, tilting of the homo-epitaxial GaP film failed to reveal any defect similar to the PDTs.

4. Discussion

When a semiconductor surface is irradiated with a laser, there is a rise in temperature. Using Thompson's model [14] the maximum temperature rise on GaP and GaAs surfaces during pulsed laser irradiation (laser pulse of 0.11 $\mathrm{J\,cm^{-2}}$) was determined to be about 1150 and 1230 K, respectively, with the substrate heated externally to 500 °C. The model also predicts that a significant temperature rise occurs in GaP to a depth of under 0.1 μm, whereas in GaAs, this value is slightly over 0.1 μm. Such high temperatures persist in the solids for a fraction of a ms after each pulse. This means that both the thin film and the substrate experienced rapid heating and cooling during continuous laser pulsing during growth. Such rapid thermal cycle processing can lead to stresses in both the film and the substrate. This is expected to be particularly severe in the hetero-epitaxial growth of GaP on GaAs, because of the thermal expansion coefficient mismatch between the film and the substrate.

During the hetero-epitaxial growth of GaP, there are at least two sources of defects at the interface. First, there is a 4% lattice mismatch which gives rise to line and planar defects. Most of these defects are accommodated at the heterojunction interface. The second source of defects originate due to initial composition inhomogeneities during the nucleation stage. These could lead to atomic deposition errors resulting in a high density of planar defects (i.e., twins) at the interface. Thus a highly defective region consisting of microtwins and dislocations is formed near the interface during the initial stages of hetero-epitaxial growth. These microtwins are believed to be sustained and grown in response to the thermal expansion mismatch induced stress. In a conventional thermal epitaxial growth process, heating of the substrate is constant during growth, however in the laser-assisted process discussed here, the substrate and the film are subjected to repeated heating and cooling cycles. Such rapid thermal cycling is expected to aggravate the stress induced because of the thermal expansion mismatch between the film and the substrate. In the case of homo-epitaxy, propagation of microtwins was not observed due to similar physical properties of the film and the substrate in spite of rapid thermal cycles during growth. In the absence of the laser light, as mentioned above, the growth was fine grained polycrystalline, and thus, it is evident that the thermal contribution from the laser plays an important role in the growth process.

5. Conclusion

We have examined the crystalline defects in laser-assisted homo- and hetero-epitaxy of GaP using XTEM. The dominant defects in homo-epitaxial growth are stacking faults compared to twins in hetero-epitaxy. It is interesting to note that although laser-assisted epitaxy is believed to be a low temperature process, its thermal contribution appears to play an important role in inducing partial dislocations and propagation of planar defects.

Acknowledgements

The authors wish to acknowledge T. Dosluoglu for helpful discussions.

References

1. H. HEINEKE, A. BRAUERS, H. LUTH and P. BALK, *J. Cryst. Growth* **77** (1986) 241.
2. S. SAKAI, S. YAMAMOTO and M. UMENO, *Jpn. J. Appl. Phys.* **25** (1986) 1156.
3. J. HAIGH, *J. Vac. Sci. Technol.* **B3** (1985) 1456.

4. V. MCCRARY, V. M. DONNELLY, D. BRASEN, A. APPELBAUM and R. C. FARROW, *Mater. Res. Soc. Symp. Proc.* **75** (1987) 223.
5. H. KUKIMOTO, Y. BAU, H. KOMATSU, M. TAKECHI and M. ISHIGAKI, *J. Cryst. Growth* **77** (1986) 223.
6. V. M. DONNELLY, D. BRASEN, A. APPLEBAUM and M. GEVA, *J. Appl. Phys.* **58** (1985) 2202.
7. S. S. CHU, T. L. CHU, C. L. CHANG and H. FIROUZI, *Appl. Phys. Lett.* **52** (1988) 1243.
8. B. J. MORRIS, *ibid.* **48** (1986) 867.
9. U. SUDARSAN, N. CODY, T. DOSLOGLU and R. SOLANKI in Proceedings of the Materials Research Society Fall Meeting MA (Boston, MRS. 1988) Vol. 129 p. 321.
10. *Idem., Appl. Phys. A, Appl. Phys. A,* **50,** (1990) 325.
11. P. HIRSCH, A. HOWIE, R. B. NICHOLSON, D. W. PASHLEY and M. J. WHELAN, in "Electron Microscopy of Thin crystals" (Butterworths, London, 1967) p. 234.
12. S. N. G. CHU, W. T. TSANG, T. H. CHIU and A. T. MACRANDER, *J. Appl. Phys.* **66** (1989) 520.
13. S. N. G. CHU, S. NAKAHARA, R. F. KARLICEK, K. E. STREGE, D. MITCHAM and W. D. JOHNSTON Jr., *J. Appl. Phys.* **64** (1988) 2523.
14. M. O. THOMPSON, Ph.D. thesis, Cornell University New York (1984).

Received 14 November 1989
and accepted 6 February 1990